

The C-terminal Tail of CRTH2 Is a Key Molecular Determinant That Constrains $G\alpha_i$ and Downstream Signaling Cascade Activation^{*□}

Received for publication, September 4, 2008, and in revised form, October 26, 2008. Published, JBC Papers in Press, November 14, 2008, DOI 10.1074/jbc.M806867200

Ralf Schröder[‡], Nicole Merten[‡], Jesper Mosolff Mathiesen[§], Lene Martini[¶], Anamarija Kruljac-Letunic^{||}, Friederike Krop^{||}, Andree Blaukat^{||}, Ye Fang^{**}, Elizabeth Tran^{**}, Trond Ulven^{††}, Christel Drewke[‡], Jennifer Whistler[¶], Leonardo Pardo^{§§}, Jesús Gomeza[‡], and Evi Kostenis^{‡1}

From the [‡]Institute of Pharmaceutical Biology, University of Bonn, Nussallee 6, 53115 Bonn, Germany, the [§]Department of Molecular Pharmacology, Zealand Pharma A/S, Smedeland 26B, DK-2600 Glostrup, Denmark, the [¶]Ernest Gallo Clinic and Research Center, University of California, San Francisco, Emeryville, California 94608, ^{||}TA Oncology, Merck Serono Research, Merck KGaA, Frankfurter Strasse 250, 64293 Darmstadt, Germany, ^{**}Biochemical Technologies, Science and Technology Division, Corning Inc., Corning, New York 14831, the ^{††}Department of Physics and Chemistry, University of Southern Denmark, Campusvej 55, DK-5230 Odense, Denmark, the ^{§§}Laboratorio de Medicina Computacional, Unitat de Bioestadística, Facultat de Medicina, Universitat Autònoma de Barcelona, 08193 Bellaterra, Spain

Prostaglandin D₂ activation of the seven-transmembrane receptor CRTH2 regulates numerous cell functions that are important in inflammatory diseases, such as asthma. Despite its disease implication, no studies to date aimed at identifying receptor domains governing signaling and surface expression of human CRTH2. We tested the hypothesis that CRTH2 may take advantage of its C-tail to silence its own signaling and that this mechanism may explain the poor functional responses observed with CRTH2 in heterologous expression systems. Although the C terminus is a critical determinant for retention of CRTH2 at the plasma membrane, the presence of this domain confers a signaling-compromised conformation onto the receptor. Indeed, a mutant receptor lacking the major portion of its C-terminal tail displays paradoxically enhanced $G\alpha_i$ and ERK1/2 activation despite enhanced constitutive and agonist-mediated internalization. Enhanced activation of $G\alpha_i$ proteins and downstream signaling cascades is probably due to the inability of the tail-truncated receptor to recruit β -arrestin2 and undergo homologous desensitization. Unexpectedly, CRTH2 is not phosphorylated upon agonist-stimulation, a primary mechanism by which GPCR activity is regulated. Dynamic mass redistribution assays, which allow label-free monitoring of all major G protein pathways in real time, confirm that the C terminus inhibits $G\alpha_i$ signaling of CRTH2 but does not encode G protein specificity determinants. We propose that intrinsic CRTH2 inhibition by its C terminus may represent a rather unappreciated strategy employed by a GPCR to specify the extent of G protein activation and that this mechanism may compensate for the absence of the classical phosphorylation-dependent signal attenuation.

Prostaglandin D₂ (PGD₂)² is a lipid mediator that has been considered essential in the development of inflammatory diseases such as asthma and atopic dermatitis (1–3). It is the major cyclooxygenase metabolite synthesized in allergen-activated mast cells and is released upon their immunological activation (4). The biological effects of PGD₂ are mediated by two G protein-coupled receptors, DP1 and DP2/CRTH2 (chemoattractant receptor homologous molecule expressed on T helper type 2 cells), respectively (5, 6). DP1 activation leads to $G\alpha_s$ -mediated elevation of intracellular cyclic AMP, whereas activation of CRTH2 results in an increase in intracellular Ca²⁺ levels via the $G\alpha_i$ pathway and a decrease in cAMP, but also G protein-independent, arrestin-mediated cellular responses have been observed (5–7).

CRTH2 in particular is expressed on eosinophils, basophils, and T helper type 2 lymphocytes. Activation by PGD₂ or its active metabolites transduces the chemokinetic activity on these immune cells and, by doing so, mediates their recruitment to sites of inflammation (2, 3, 6, 8–13). In mouse models of allergic asthma or atopic dermatitis, CRTH2 activation promotes eosinophilia and exacerbates pathology (14–17). In humans, the proinflammatory role of CRTH2 is underscored by the finding that sequence variants conferring enhanced mRNA stability onto the receptor are associated with a higher degree of bronchial hyperreactivity and the occurrence of fatal asthma (16).

Notably, since deorphanization of CRTH2 in 2001 (6), quite a number of reports became available highlighting a proinflammatory role for this receptor in native cells and animal models as well as in humans (2, 3, 6, 8–13, 16, 18–22). In contrast, no study has yet addressed structure function relationships of CRTH2 in recombinant cells, and only a single report addresses this topic for the mouse CRTH2 receptor (23). In fact, molecu-

* The costs of publication of this article were defrayed in part by the payment of page charges. This article must therefore be hereby marked "advertisement" in accordance with 18 U.S.C. Section 1734 solely to indicate this fact.

□ The on-line version of this article (available at <http://www.jbc.org>) contains supplemental Figs. 1 and 2.

¹ To whom correspondence should be addressed: Institute for Pharmaceutical Biology, Dept. of Molecular, Cellular, and Pharmacobiology, University of Bonn, Nussallee 6, 53115 Bonn, Germany. Tel.: 49-228-732678/733194; Fax: 49-228-733250; E-mail: kostenis@uni-bonn.de.

² The abbreviations used are: PGD₂, prostaglandin D₂; BRET, bioluminescence resonance energy transfer; DMR, dynamic mass redistribution; EGF, epidermal growth factor; ELISA, enzyme-linked immunosorbent assay; ERK, extracellular signal-regulated kinase; GPCR, G protein-coupled receptor; GTP γ S, guanosine 5'-O-(3-thiotriphosphate); Hx8, helix 8; IP, inositol phosphate; MAPK, mitogen-activated protein kinase; PTX, pertussis toxin; Rluc, Renilla luciferase; WT, wild type; HBSS, Hanks' balanced saline solution.

lar determinants that govern expression, regulation, signaling, or trafficking of human CRTH2, knowledge that could aid in the development of novel therapeutic principles to combat allergic diseases, have yet to be fully elucidated. We suggest that this dearth of information may be due, at least in part, to the poor functional performance of CRTH2 in recombinant expression systems, which are required to study receptor behavior of wild type and genetically engineered variants. During the course of our study, we were intrigued by the poor efficacy of PGD₂ causing rather miniscule receptor activation as compared with other *bona fide* G_{i/o}-selective receptors. In an attempt to understand the regulatory mechanisms that define the extent of CRTH2 signaling, we have identified the C-terminal tail region of CRTH2 as a key molecular determinant that constrains G protein-dependent signaling events. We propose that CRTH2 utilizes its C-terminal tail to limit acute or chronic overstimulation and that this mechanism might compensate for the absence of the classical negative feedback regulation, which is dependent on the concerted action of G protein-coupled receptor kinases, second messenger-dependent kinases, and arrestin proteins.

EXPERIMENTAL PROCEDURES

Materials and Reagents—Tissue culture media and reagents were purchased from Invitrogen. Epic[®] biosensor microplates (cell culture-compatible) and compound source plates were from Corning Inc. 5-Oxo-eicosatetraenoic acid, PGD₂ (Biozol), [³H]PGD₂, [³⁵S]GTP-γS (PerkinElmer Life Sciences), mouse M1 monoclonal antibody, poly-D-lysine (Sigma), Alexa Fluor 488-conjugated goat anti-mouse IgG_{2b} antibody (Invitrogen), nicotinic acid (Sigma), and interleukin-8 (PeproTech EC) were purchased as indicated. All other laboratory reagents were from Sigma unless explicitly specified. Synthesis of the CRTH2 antagonist TRQ11238 was described previously (24). Chemerin was a kind gift of Professor Girolamo Calo (University of Italy and UFPeptides, Ferrara).

DNA Constructs—The coding sequence of human CRTH2 (GenBank[™] accession number NM_004778) was amplified by PCR from a human hippocampus cDNA library and inserted into the pcDNA3.1(+) expression vector (Invitrogen) via 5' HindIII and 3' EcoRI. To create a mutant CRTH2 receptor lacking the entire C terminus except for the putative helix 8 (herein referred to as CRTH2 ΔCtail), a STOP codon was introduced by PCR mutagenesis after amino acid Arg³¹⁷, and the truncated receptor was cloned into pcDNA3.1(+) via 5' HindIII and 3' EcoRI. Construction of the chimeric G protein Gα_qG66Di5 in the pcDNA3.1(+) ZEO expression vector was reported previously (25). The high affinity nicotinic acid receptor HM74a (26) was cloned from adipose tissue and inserted into pcDNA3.1(+) via HindIII/EcoRI sites. The OXE receptor (27) and the chemerin receptor ChemR23 (28) were cloned from human leukocyte cDNA and inserted via 5' HindIII, 3' EcoRI and 5' BamHI, 3' EcoRI, respectively, into pcDNA3.1(+). Correctness of the constructs was verified by restriction endonuclease digestion and sequencing in both directions (MWG Biotech, Ebersberg, Germany).

Cell Culture and Transfection—COS-7 and HEK293 cells were grown in Dulbecco's modified Eagle's medium supple-

mented with 10% (v/v) heat-inactivated fetal calf serum, 1% sodium pyruvate, 100 units/ml penicillin, and 100 μg/ml streptomycin and kept at 37 °C in a 5% CO₂ atmosphere. To facilitate functional analysis of CRTH2 wild type (WT) and CRTH2 ΔCtail, respectively, stable HEK293 cell clones were established using media containing 500 μg/ml G418 and the FLAG-tagged versions of the receptors. For transient transfections, the calcium phosphate DNA precipitation method was used as previously described (7). For functional inositol phosphate assays, HEK293 cells were transiently cotransfected with CRTH2 WT or CRTH2 ΔCtail and a promiscuous Gα protein facilitating inositol phosphate production by a G_i-selective CRTH2 receptor (25).

Membrane Preparation—48 h after transfection, HEK293 cells were harvested, and cell pellets were resuspended in an ice-cold buffer containing 20 mM HEPES and 10 mM EDTA. Then cells were ruptured using Dounce homogenization. Nuclei were pelleted (800 × g, 10 min, 4 °C), and the post-nuclear supernatant was then fractionated (30,000 × g, 30 min, 4 °C) into membrane pellets and supernatants. Pellets were resuspended in buffer containing 20 mM HEPES, 0.1 mM EDTA, and a protease inhibitor mixture (Roche Applied Science) and stored at -80 °C. Membrane protein concentrations were quantified with protein assay kit (Pierce) using bovine serum albumin as a standard.

Whole Cell Binding Experiments—24 h after transfection, HEK293 cells were seeded into poly-D-lysine-coated 96-well plates at a density of 30,000 cells/well. Competition binding experiments on whole cells were then performed ~18–24 h later using 1.0 nM [³H]PGD₂ (172 Ci/mmol; PerkinElmer Life Sciences) in a binding buffer consisting of HBSS and 10 mM HEPES, pH 7.5. Total and nonspecific binding were determined in the absence and presence of 10 μM PGD₂, respectively. Binding reactions were conducted for 3 h at 4 °C and were terminated by two washes (100 μl each) with ice-cold binding buffer. Radioactivity was determined by liquid scintillation counting in a TopCount liquid scintillation counter (PerkinElmer Life Sciences) (27% counting efficiency) after overnight incubation in MicroScint 20. Binding assays using stable HEK293 cell clones were performed as described above. Saturation binding analysis on stable HEK293 cell clones was performed essentially as described previously (7). Briefly, increasing concentrations of [³H]PGD₂ (specific activity 172 Ci/mmol) were incubated with cells for 3 h at 4 °C in the absence or presence of 10 μM unlabeled PGD₂.

Membrane Binding Experiments—Cell membranes from transiently transfected HEK293 cells (15 μg of protein) were incubated with 1.0 nM [³H]PGD₂ (172 Ci/mmol) in a binding buffer consisting of HBSS and 100 mM HEPES (pH 7.4) under continuous shaking at 4 °C for 3 h. Total and nonspecific binding were determined in the absence and presence of 10 μM PGD₂, respectively. For inhibition of binding by GTP, varying concentrations of GTP were added to the binding mixture. The receptor-bound radioligand was filtered on a Tomtech 96-well Mach III Harvester (PerkinElmer Life Sciences) using filters presoaked with 0.1% polyethyleneimine (Filtermat A; PerkinElmer Life Sciences). Filtration was immediately followed by three rinses with ice-cold 100 mM NaCl. Thereafter,

Silencing of CRTH2 Signaling by Its C-terminal Tail

scintillation wax (Meltilex A; PerkinElmer Life Sciences) was melted onto the dried Filtermat. The filters were placed in sample bags (PerkinElmer Life Sciences), and filter-bound radioactivity was measured using a Microbeta Trilux-1450 scintillation counter (PerkinElmer Life Sciences). Determinations were made in triplicates in two independent experiments.

[³⁵S]GTPγS Binding Assays—Scintillation proximity assays were carried out using 15 μg of membrane protein in GTPγS binding buffer (50 mM HEPES, pH 7.5, 100 mM NaCl, 5 mM MgCl₂, 0.1% bovine serum albumin, and 10 μg/ml saponin) with 50 nCi of [³⁵S]GTPγS, 1 μM GDP, and 0.4 mg of wheat germ agglutinin-coupled scintillation proximity assay beads (RPNQ0001; GE Healthcare), as described before (29).

Inositol Phosphate (IP) Accumulation Assays—24 h after transfection, cells were seeded in poly-D-lysine-coated 96-well tissue culture plates and loaded with 0.5 μCi of [2-³H]myo-inositol (TRK911; Amersham Biosciences). The next day, cells were washed twice in HBSS buffer (including CaCl₂ and MgCl₂) and stimulated with the respective agonists in HBSS buffer supplemented with 10 mM LiCl for 45 min at 37 °C. The reactions were terminated by aspiration and the addition of 50 μl of 10 mM ice-cold formic acid/well. After a 90-min incubation on ice, 20 μl of the resulting cell extract was transferred to 80 μl of yttrium silicate scintillation proximity assay beads (12.5 mg/ml; Amersham Biosciences), and shaken for 60 min at 4 °C. Yttrium silicate beads were centrifuged to settle and incubated overnight at 4 °C before counting on a TopCount microplate scintillation counter.

cAMP Accumulation Assays—Inhibition of forskolin-stimulated cAMP accumulation in HEK293 cells stably expressing either CRTH2 WT or CRTH2 ΔCtail was performed using the HTRF[®]-cAMP dynamic kit (CIS Bio International, Gif-sur-Yvette cedex, France). In brief, cells were resuspended in assay buffer (HBSS, 20 mM HEPES, 1 mM 3-isobutyl-1-methylxanthine) and dispensed in 384-well microplates at a density of 50,000 cells/well. After preincubation in assay buffer for 30 min, cells were stimulated with PGD₂ in the presence of 5 μM forskolin for 30 min at room temperature. The reactions were stopped by the addition of 50 mM phosphate buffer (pH 7.0), 1 M KF, and 1.25% Triton X-100 containing HTRF[®] assay reagents. The assay was incubated 60 min at room temperature, and time-resolved FRET signals were measured after excitation at 320 nm using the Mithras LB 940 multimode reader (Berthold Technologies, Bad Wildbad, Germany). Data analysis was made based on the fluorescence ratio emitted by labeled cAMP (665 nm) over the light emitted by the europium cryptate-labeled anti-cAMP (620 nm). Levels of cAMP were normalized to the amount of cAMP elevated by 5 μM forskolin alone.

Bioluminescence Resonance Energy Transfer (BRET) Assay—BRET assays were performed on HEK293 cells transiently transfected to co-express human CRTH2-Rluc or CRTH2 ΔCtail-Rluc and β-arrestin2-GFP2 (green fluorescent protein 2) fusion proteins, using the Mithras LB 940 microplate reader (Berthold Technologies), as described previously (29). In brief, 5 s after the simultaneous addition of agonist and Deep Blue C, light output was measured sequentially at 400 and 515 nm, and the BRET signal (mBRET ratio) was calculated as the ratio

of the fluorescence emitted by β-arrestin2-GFP2 (515 nm) over the light emitted by the receptor-Rluc (400 nm).

Enzyme-linked Immunosorbent Assay (ELISA)—24 h after transfection, cells were seeded in poly-D-lysine-coated 48-well tissue culture plates at a density of 100,000 cells/well. The next day, cells were fixed with 4% paraformaldehyde, washed three times with phosphate-buffered saline, and blocked with blocking buffer (3% dry milk, 50 mM Tris-HCl, pH 7.5). For cells expressing the untagged CRTH2 WT or CRTH2 ΔCtail, the primary monoclonal rat anti-CRTH2 antibody (BM16, sc-21798; Santa Cruz Biotechnology, Inc., Santa Cruz, CA) and the secondary goat anti-rat horseradish peroxidase-conjugated antibody (sc-2006; Santa Cruz Biotechnology) were used. Cells expressing the N-terminally FLAG-tagged CRTH2 WT or CRTH2 ΔCtail were incubated with the monoclonal mouse anti-FLAG M1 antibody (Sigma) and goat anti-mouse horseradish peroxidase-conjugated secondary antibody (Bio-Rad). Primary antibodies were used as 1:500 dilutions and secondary antibodies as 1:2500 dilutions in blocking buffer. Colorimetric readings were obtained using the horseradish peroxidase-substrate 3,3',5,5'-tetramethylbenzidine (Sigma) on the Tecan Sunrise reader (Tecan, Switzerland) at 450 nm.

Immunocytochemistry—Cells stably expressing either CRTH2 WT or CRTH2 ΔCtail were grown on poly-D-lysine-treated coverslips. When reaching ~50% confluence, the cells were incubated with M1 antibody directed against the N-terminal FLAG-epitope (1:1,000) for 30 min at 37 °C and subsequently fixed in 4% formaldehyde in phosphate-buffered saline. A subset of cells were treated with 10 μM PGD₂ or left untreated for another 30 min before fixation. Following three washes in TBSC (137 mM NaCl, 25 mM Tris-base, 3 mM KCl, 1 mM CaCl₂), the cells were permeabilized in blotto (3% milk, 0.1% Triton X-100, 50 mM Tris-HCl, pH 7.5), stained with Alexa Fluor 488-conjugated goat anti-mouse IgG2b antibody (1:500, 20 min), washed three times in TBSC, and mounted on glass microslides using Vectashield mounting medium.

Biotin Protection Degradation Assay—HEK293 cells stably expressing CRTH2 WT or CRTH2 ΔCtail were grown to confluence in poly-D-lysine-pretreated 10-cm plates. Cells were treated with 0.3 mg/ml disulfide-cleavable biotin (Pierce) at 4 °C for 30 min and washed in TBSC (137 mM NaCl, 25 mM Tris-base, 3 mM KCl, 1 mM CaCl₂). Cells were then incubated at 37 °C in Dulbecco's modified Eagle's medium for 20 min before adding 10 μM PGD₂ or left untreated for another 30 min. The two control plates, 100% and strip, remained at 4 °C in TBSC. Except for the 100% plate, all plates were washed in phosphate-buffered saline, and remaining cell surface bound biotin was removed in strip buffer (50 mM glutathione, 75 mM NaCl, 75 mM NaOH, 1% fetal bovine serum) at 4 °C for 30 min. All plates were then quenched in buffer containing 9 mg/ml iodoacetamide and 10 mg/ml bovine serum albumin at 4 °C for 20 min, followed by cell lysis in IPB (150 mM NaCl, 25 mM KCl, 10 mM Tris-HCl, 1 mM CaCl₂, 0.1% Triton X-100, pH 7.4, with added protease inhibitors (Complete; Roche Applied Science) and 1 mg/ml iodoacetamide). Cellular debris was removed by centrifugation at 10,000 × g at 4 °C for 10 min, and lysates were immunoprecipitated with anti-FLAG M2 antibodies linked with rabbit anti-mouse linker antibodies to Protein A-Sepharose beads

at 4 °C, washed extensively, and treated with peptide:N-glycanase F at 37 °C for 1 h. Samples were denatured in nonreducing SDS sample buffer, resolved by SDS-PAGE using 4–20% Tris-glycine precast gels (Invitrogen), transferred to nitrocellulose membrane, overlaid with streptavidin (Vectastain ABC immunoperoxidase reagent; Vector Laboratories), and developed with ECL plus reagents (Amersham Biosciences).

Dynamic Mass Redistribution (DMR) Assays (Corning Epic® Biosensor Measurements)—A beta version of the Corning® Epic® system was used, consisting of a temperature control unit, an optical detection unit, and an on-board robotic liquid handling device. Briefly, each well in the 384-well Epic® microplate contains a resonant wave guide grating biosensor. The system measures changes in the local index of refraction upon mass redistribution within the cell monolayer grown on the biosensor. Ligand-induced DMR in living cells is manifest as a shift in the wavelength of light that is reflected from the sensor. The magnitude of this wavelength shift is proportional to the amount of DMR. Increase of mass contributes positively and decrease contributes negatively to the overall response. For the Epic® system, the penetration depth is 150 nm (*i.e.* DMR that takes place within penetration depth can be detected) (30, 31). 24 h before the assay, HEK293 cells were seeded onto fibronectin-coated 384-well Epic® sensor microplates at a density of 15,000 cells/well and cultured for 20–24 h (37 °C, 5% CO₂) to obtain confluent monolayers. After the removal of medium, cells were washed with HBSS containing 20 mM HEPES and kept for 1 h in the Epic® reader at a constant temperature of 28 °C. Hereafter, the sensor plate was scanned, and a base-line optical signature was recorded. Then compound solutions were transferred into the sensor plate, and DMR was monitored for at least 3000 s.

ERK/MAPK Activation—HEK293 cells stably expressing CRTH2 WT or CRTH2 Δ Ctail were cultured to confluence and then starved in serum-free Dulbecco's modified Eagle's medium overnight with one change of starvation medium after 1.5 h. Cells were treated for 16 h with pertussis toxin (PTX) (Calbiochem) or for 50 min with different inhibitors (bisindolylmaleimide I (Calbiochem), PP2 (Calbiochem), AG 1478 (Calbiochem), Iressa (Astra Zeneca), or the CRTH2-specific arrestin translocation inhibitor (compound 1 in Ref. 7, herein referred to as 27868)) and stimulated for 10 min with 10 μ M PGD₂. Following aspiration, cells were frozen in liquid nitrogen and lysed, and lysates were subjected to SDS-PAGE and Western blot analysis as described previously (32).

Receptor Phosphorylation—Receptor phosphorylation was analyzed as previously described (33, 34). Briefly, confluent HEK293 cells grown in 6-well plates were transfected with 1.5 μ g/well plasmid DNA of empty expression vector, CRTH2 WT, CRTH2 Δ Ctail, or control protein that is known to be highly phosphorylated (ASAP1) (32); all proteins were FLAG-tagged. 24 h after transfection, cells were washed twice with phosphate-free HEPES-buffered Dulbecco's modified Eagle's medium and labeled in the same medium with 0.5 mCi/ml [³²P]orthophosphate for 6 h. Following a 5-min stimulation with increasing concentrations of PGD₂, cells were lysed in 1 ml of ice-cold radioimmune precipitation buffer containing protease and phosphatase inhibitor mixtures (Calbiochem), and FLAG-

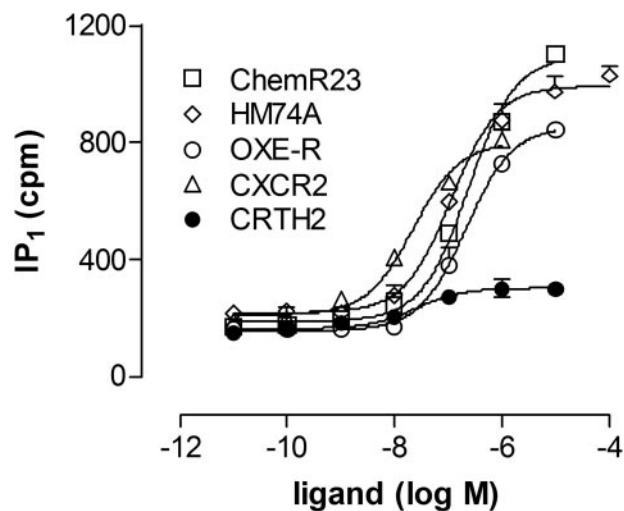


FIGURE 1. Signaling efficacy of CRTH2 WT is poor compared with other *bona fide* G_{i/o}-selective receptors. HEK293 cells were transiently transfected with the indicated receptors and a chimeric G_α_iG66Di5 protein (25) that funnels G_i-selective receptors to the G_q pathway. Cells were treated with increasing agonist concentrations for 45 min and assayed for total IP accumulation, as described in detail under "Experimental Procedures." The following agonists were used: chemerin for ChemR23, nicotinic acid for HM74A, 5-oxo-eicosatetraenoic acid for the OXE receptor, interleukin-8 for the chemokine receptor CXCR2, and PGD₂ for CRTH2. Data (mean ± S.E., *n* = 3) are representative of experiments repeated on three separate occasions.

tagged proteins were isolated with an anti-FLAG monoclonal antibody precoupled to agarose beads (Sigma) under gentle shaking for 3 h at 4 °C. Beads were washed three times with lysis buffer, and proteins were released with SDS sample buffer and a 5-min incubation at 98 °C. Samples were subjected to SDS-PAGE, transferred to nitrocellulose membranes, and analyzed using a phosphor imaging system (BAS-2000; Fuji). To control expression of CRTH2 proteins, the same nitrocellulose membranes were probed with an anti-FLAG monoclonal antibody (Sigma).

Calculations and Data Analysis—IC₅₀ and EC₅₀ values were determined by nonlinear regression using Prism 4.02 (GraphPad Software, Inc.). Values of the dissociation and inhibition constants (*K_d* and *K_i*) were estimated from competition binding experiments using the equations $K_d = IC_{50} - L$ and $K_i = IC_{50}/(1 + L/K_d)$, where *L* is the concentration of radioactive ligand and *K_d* is its dissociation constant.

RESULTS

The C-terminal Tail of CRTH2 Is Important for Cell Surface Expression—Analysis of CRTH2 receptor function in transiently transfected cells is hampered by the poor responses generated upon PGD₂ stimulation. In fact, comparison of the signaling capabilities of a set of *bona fide* G_{i/o}-coupled receptors in second messenger assays reveals that CRTH2 is functionally expressed but that the efficacy of activation is significantly smaller as compared with other G_i-selective receptors, such as the Chemerin receptor ChemR23, the nicotinic acid receptor HM74A, the 5-oxo-eicosatetraenoic acid receptor OXE, or the chemokine receptor CXCR2 (Fig. 1). C termini have emerged as a crucial region of GPCRs governing various aspects of their function, such as expression (35, 36), dimerization (37), signaling (36, 38–40), trafficking (35, 36, 41), and binding to regula-

Silencing of CRTH2 Signaling by Its C-terminal Tail

tory proteins of the arrestin family (40–43). Herein, we tested the hypothesis that the C terminus of CRTH2 may serve to constrain receptor signaling. To this end, a CRTH2 truncation mutant was created (hereafter referred to as Δ Ctail) by cDNA deletion. The mutant protein was terminated at position 317 to remove the major portion of the C-terminal tail except for the domain that contains functionally important residues of the putative cytoplasmic helical structure termed helix 8 (Hx8) (Fig. 2A). Hx8 is adjacent to transmembrane domain VII and thought to be present in most if not all family A GPCRs (44–47). Sequence alignments of Δ Ctail with selected GPCRs, crystal structures of which are available (Fig. 2B), and a molecular model of the Δ Ctail region forming the end of TM7 (transmembrane 7) and the predicted Hx8 (Fig. 2C) show that this construct retains all of the important elements of Hx8 that permit interaction with TM7, the adjacent intracellular loop 1 as well as the C-terminal domain of $G\alpha_i$. The presence of these structural features is important, since their integrity has been shown to be crucial for proper receptor function (38, 39, 41, 45, 48–53). The effect of C-terminal truncation on CRTH2 surface expression was assessed in whole cell ligand binding assays utilizing [3 H]PGD₂. Although surface expression was significantly reduced for the tail-truncated receptor (Fig. 2D), C-tail deletion was accompanied by an increased affinity of the receptor for its agonist PGD₂, which in turn might be indicative of an intrinsic inhibitory role of the C-tail. To verify that the observed reduction in binding sites reflected an actual decrease of total receptor number at the cell surface, WT and mutant receptor expression was analyzed by an ELISA (Fig. 2E). ELISA analysis confirmed a reduction in total receptor numbers for Δ Ctail. To facilitate analysis of receptor behavior in subsequent studies, stable cell lines expressing FLAG-tagged WT and Δ Ctail receptors were generated, and isolated clones were selected to resemble receptor expression under transient conditions (Fig. 2, F and G). Introduction of N-terminal FLAG tags did not affect [3 H]PGD₂ pharmacology of CRTH2 WT and Δ Ctail, respectively (not shown). Importantly, decrease in cell surface expression of Δ Ctail was not due to deficient cellular expression, because similar total cellular levels of WT and Δ Ctail were detected in confocal images and radioligand binding assays on membrane preparations (Fig. 3, A and B).

The CRTH2 C Terminus Is a Negative Regulator of G Protein-dependent Signaling—To assess the effect of C-tail truncation on receptor-G protein coupling, CRTH2 WT and Δ Ctail were tested for their ability to stimulate IP production in HEK293 cells transiently transfected with the receptor constructs and a chimeric G protein linking G_i -selective receptors to the G_q -phospholipase $C\beta$ pathway (Fig. 4A). Interestingly, IP production of the tail-truncated receptor was significantly increased upon PGD₂ stimulation as compared with the WT receptor. In fact, deletion of the tail appears to paradoxically enhance receptor signaling and suggests that the tail may act to constrain maximum receptor function. Functional superiority of the Δ Ctail is not due to altered affinity of PGD₂ for the receptor in the presence of the chimeric G protein (supplemental Fig. 1A) or to altered surface expression due to G protein cotransfection (supplemental Fig. 1B). Enhancement by tail deletion of receptor signaling was also observed in COS-7 cells, excluding the

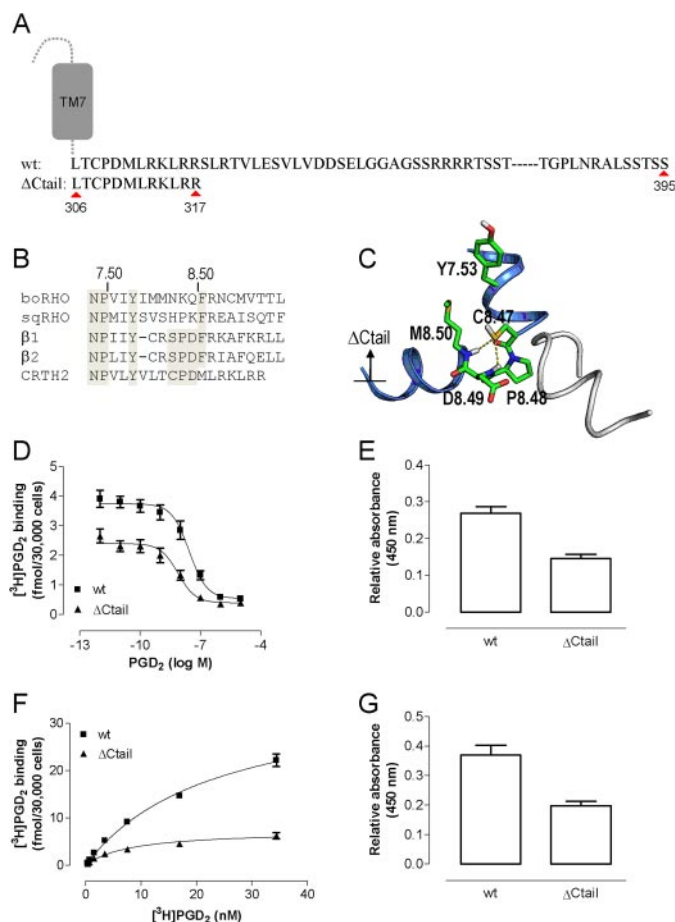


FIGURE 2. The CRTH2 C terminus is important for cell surface expression.

A, architecture of CRTH2 WT and the CRTH2 Δ Ctail construct. The amino acid sequence of the CRTH2 C terminus downstream of the predicted seventh transmembrane domain is listed. Residue numbers of amino acids are shown below the sequence, and the position of truncation is indicated. Omitted amino acids are indicated by a dashed line. CRTH2 Δ Ctail is lacking the entire intracellular C terminus except for the important structural features of the putative eighth helix. B, sequence alignments of the amino acids forming the end of TM7 and Hx8 for bovine (*boRHO*) and squid (*sqRHO*) rhodopsin, β_1 - and β_2 -adrenergic (β_2 -AR) receptors, and Δ Ctail of CRTH2. Conserved residues of the NPXXY motif of TM7 and Hx8 are boxed. (Residue numbering according to Ref. 78.) C, molecular model of TM7 and Hx8 of CRTH2 Δ Ctail (blue traces), constructed from the crystal structures of bovine rhodopsin and the β_2 -adrenergic receptor. CRTH2 possesses the CPD motif comparable with the SPD motif of the β_2 -adrenergic receptor, in which Ser8.47³²⁹ of β_2 -adrenergic receptor or Cys8.47³⁰⁸ of CRTH2 stabilizes the backbone N-H amide atoms at the beginning of Hx8. This suggests that Hx8 of CRTH2 starts with Pro8.48³⁰⁹ at the same position as the known crystal structures. The putative orientation of the C-terminal helix of $G\alpha_i$ (white traces), as modeled from the recently obtained crystal structure of opsin in its G protein-interacting conformation (Protein Data Bank entry 3DQB), is depicted for comparison purposes. The position in which CRTH2 was truncated in the Δ Ctail deletion mutant is shown. Thus, all polar amino acids of Hx8 in the vicinity of TM1, -2, and -7; the intracellular loop 1; and the C-terminal helix of $G\alpha_i$ are maintained in the Δ Ctail construct. D, HEK293 cells transiently transfected with the indicated CRTH2 constructs were assayed for cell surface expression utilizing 1 nM [3 H]PGD₂ in homologous competition binding assays on whole cells: pIC50 WT, 7.55 \pm 0.13; pIC50 Δ Ctail, 8.11 \pm 0.16. Data are mean \pm S.E. from three independent experiments, each performed in duplicate. E, an ELISA was used to assess cell surface expression in HEK293 cells transiently transfected with the indicated receptor constructs. Data are mean \pm S.E. from five independent experiments, each performed in triplicate. F, saturation binding analysis on HEK293 cells stably expressing the N-terminally FLAG-tagged versions of CRTH2 WT and CRTH2 Δ Ctail receptors. Increasing concentrations of [3 H]PGD₂ were incubated with cells for 3 h at 4 $^{\circ}$ C in the absence or presence of 10 μ M unlabeled PGD₂. Specific binding was recalculated as fmol/30,000 cells after subtraction of nonspecific binding; B_{max} WT, 36.8 \pm 2.3 fmol/30,000 cells; K_D WT, 23.5 \pm 2.8 nM; B_{max} Δ Ctail, 7.3 \pm 0.5 fmol/30,000 cells; K_D Δ Ctail, 8.1 \pm 1.4 nM. Depicted is a representative data set performed in duplicate and given as mean \pm S.E. G, ELISA analysis of the cells utilized in F.

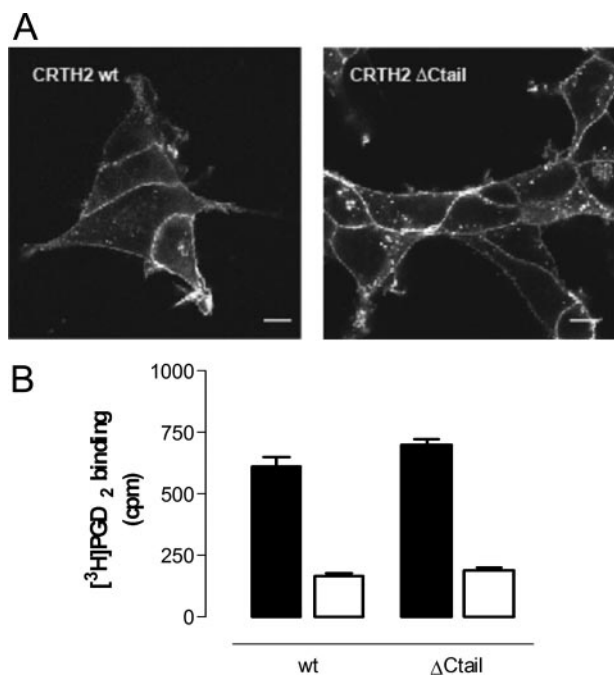


FIGURE 3. The cytoplasmic tail of CRTH2 plays an important role in regulating cellular localization. *A*, HEK293 cells stably expressing either CRTH2 WT (*left*) or CRTH2 Δ Ctail (*right*) were incubated with anti-FLAG M1 antibody recognizing a FLAG tag fused in frame to the receptor amino terminus. After incubation for 30 min at 37 °C, the cells were fixed, permeabilized, immunostained with a fluorescent secondary antibody, and imaged by confocal microscopy. This antibody "feeding" method assures exclusive labeling of receptors that are initially expressed at the cell surface and does not label intracellular, misfolded receptors. In the basal state, both CRTH2 WT and Δ Ctail were detected at the cell surface, whereas in addition the mutant receptor displayed some intracellular localization. The images shown are representative of experiments repeated on three separate occasions. Scale bar, 10 μ m. *B*, expression of CRTH2 WT or Δ Ctail receptors was assessed in membrane preparations from transiently transfected HEK293 cells using 1 nM [³H]PGD₂ in the absence (*black*) and presence (*white*) of 10 μ M PGD₂ to determine total and nonspecific binding, respectively. Data are means \pm S.E. of two independent experiments, each performed in triplicate.

possibility that functional superiority of Δ Ctail reflects an artifact of a particular cell line (Fig. 4*B*). Furthermore, comparable signaling properties of WT and Δ Ctail were also observed in functional cAMP assays, which do not require the presence of a chimeric G α protein (Fig. 4*C*). To verify differential signaling capability of the respective receptor constructs with yet another method, functional GTP γ S binding assays were performed using membranes from HEK293 cells, stably expressing CRTH2 WT and Δ Ctail, and transiently cotransfected with the G protein α subunit G α_{12} . Evidently, this biochemical signaling assay also reveals the functional superiority of Δ Ctail, since fewer receptors are sufficient to evoke the same extent of G protein activation, as observed for WT receptors (Fig. 4*D*).

Does Δ Ctail Adopt a High Affinity Conformation Even after G Protein Activation?—Exchange of GTP for GDP by the receptor-associated G protein is known to lower the receptor affinity for agonists. To test whether the functional superiority of Δ Ctail was due to its inability to switch to a low affinity conformation subsequent to G protein activation, we examined the effects of GTP on [³H]PGD₂ binding in membrane preparations from HEK293 cells transiently transfected with CRTH2 WT and Δ Ctail. GTP led to a dose-dependent decrease in high affinity agonist sites in membranes expressing CRTH2 WT

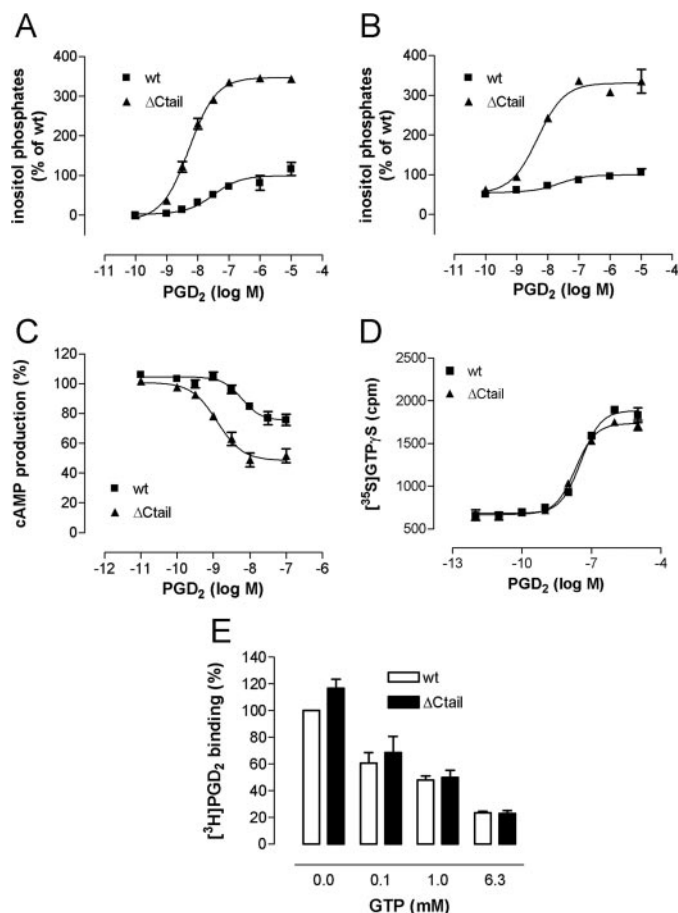


FIGURE 4. The receptor C terminus is dispensable for G protein-dependent signaling and conformational change to the low affinity state after G protein activation. *A*, HEK293 cells transiently transfected with the indicated CRTH2 receptor constructs were exposed to increasing concentrations of PGD₂ for 45 min, and the resulting increases in intracellular inositol phosphates were measured using yttrium-coated beads as described under "Experimental Procedures." *B*, IP hydrolysis assay as described in *A* in COS-7 cells transiently transfected with CRTH2 WT and Δ Ctail. *C*, inhibition of forskolin-stimulated cAMP accumulation by PGD₂. HEK293 cells stably transfected to express CRTH2 WT or Δ Ctail were stimulated with varying concentrations of PGD₂ in the presence of 5 μ M forskolin, and the resulting decrease in cAMP was measured using the HTRF[®]-cAMP dynamic kit as described under "Experimental Procedures." Data points are shown as mean values \pm S.E. of three independent experiments. *D*, [³⁵S]GTP γ S binding assay on membranes prepared from HEK293 cells stably expressing CRTH2 WT or Δ Ctail, respectively, and the G protein α subunit G α_{12} . *E*, competition for [³H]PGD₂ binding by GTP. HEK293 cells transiently transfected with CRTH2 WT and CRTH2 Δ Ctail, respectively, were harvested 48 h after transfection for membrane preparation. Fifteen μ g of membrane protein were incubated in PGD₂ binding buffer containing 1 nM [³H]PGD₂ and 0–6.3 mM GTP for 3 h at 4 °C. Membrane-bound radioactivity was measured. Data points are shown as mean values \pm S.E. of two (*E*) or three (*C*) independent experiments or individual experiments (*A*, *B*, and *D*), each representative of at least three such experiments.

(Fig. 4*E*). However, a comparable decrease in high affinity agonist sites was also observed for Δ Ctail. Hence, the functional superiority of Δ Ctail is not due to its inability to undergo a conformational change to the low affinity state after G protein activation.

Real Time Recording of CRTH2 Function Is in Agreement with GTP γ S Binding Data but Distinct from IP and cAMP Assay Outcomes—Since assays monitoring the accumulation of intracellular second messengers or membrane-based GTP γ S binding assays do not permit real time analysis of receptor signaling, we employed the novel resonant wave guide grating biosensor

Silencing of CRTH2 Signaling by Its C-terminal Tail

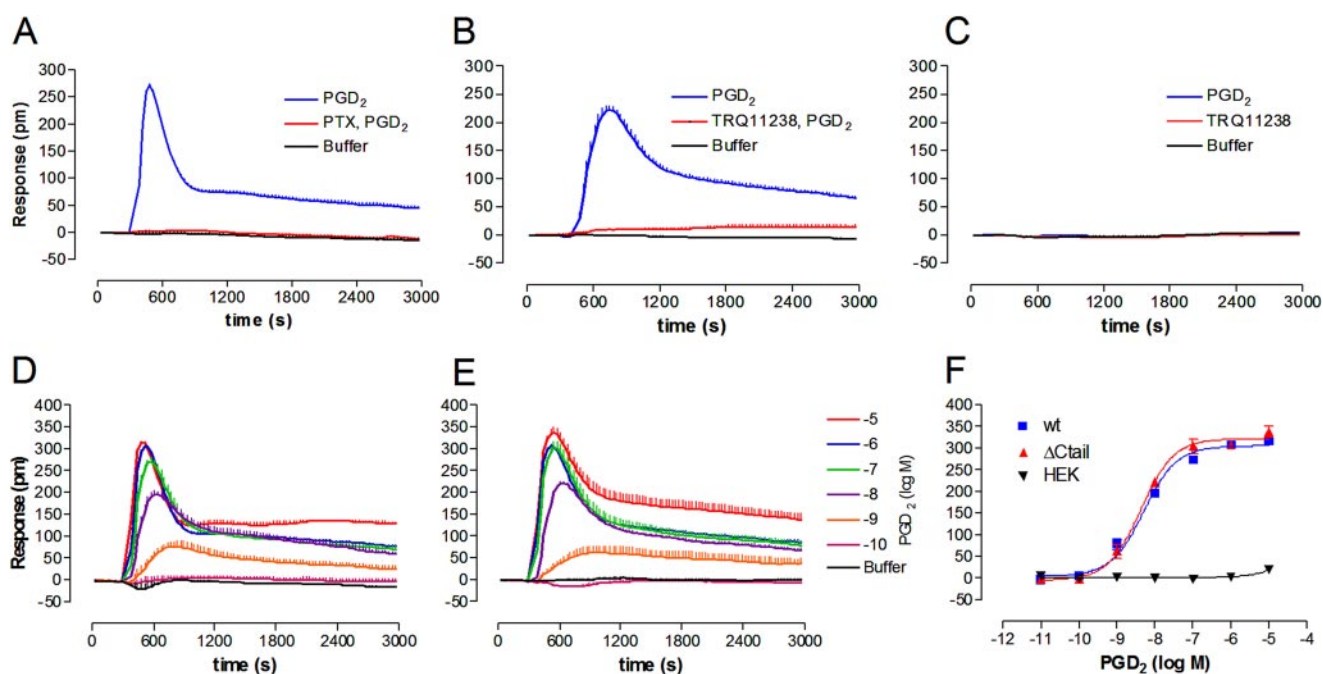


FIGURE 5. Real time analysis of receptor function confirms the inhibitory role of the C terminus for cellular signaling. HEK293 cells stably expressing CRTH2 WT or Δ Ctail, respectively, were challenged with PGD₂ in the absence and presence of the indicated inhibitors and analyzed for functional activity using real time DMR assays (Corning Epic[®] optical biosensor). DMR biosensor assays detect changes in protein relocation at the sensor surface as a function of time upon ligand stimulation. The optical signatures generated upon ligand addition faithfully reflect the G protein coupling profile of the receptor. *A*, effect of the G $\alpha_{i/o}$ inhibitor PTX (100 ng/ml, 18 h) on the specific optical signature elicited by 100 nM PGD₂ in CRTH2 WT-expressing cells. *B*, 1-h preincubation with TRQ11238, a selective CRTH2 antagonist, abolishes the specific optical signature elicited with 1 μ M PGD₂ in CRTH2 WT-expressing cells. *C*, lack of DMR signal in vector-transfected HEK293 cells upon stimulation with 1 μ M PGD₂ or 10 μ M of TRQ11238. *D* and *E*, CRTH2 WT-expressing (*D*) or CRTH2 Δ Ctail-expressing (*E*) cells were exposed to increasing concentrations of PGD₂, and agonist-mediated optical signatures were recorded as a measure of receptor functionality. *F*, concentration-response curves derived from the optical signatures in *D* and *E*, utilizing the peak maxima between the 300 and 1000 s time points are superimposable for WT and Δ Ctail, respectively. Shown are mean values \pm S.E. of representative optical recordings (*A–E*) or mean values \pm S.E. (*F*) of one experiment, representative for three such experiments, each performed in triplicate.

technology (Corning Epic[®]) to resolve signaling capability of CRTH2 WT and Δ Ctail in real time. In contrast to all other optical studies involving FRET or BRET approaches, this novel biosensor does not require introduction of any label into proteins. As such, this method is noninvasive and label-free and minimizes artifacts due to protein tagging. Activation of GPCRs is known to cause translocation of multiple signaling molecules upon receptor stimulation, and this DMR of cellular matters is captured as an optical signature. Of note, activation of the major G protein signaling pathways engaged by receptors from different coupling classes (G_{1/o}, G_s, and G_{q/11}) yield pathway-specific optical signatures (54, 55). HEK293 cells transiently transfected with CRTH2 WT or Δ Ctail, respectively, responded with specific optical signatures when exposed to increasing concentrations of PGD₂. These signatures are unequivocally due to activation of the G_i-sensitive CRTH2 receptor, since (i) they are completely abrogated when cells are pretreated with the G $\alpha_{i/o}$ inhibitor PTX (Fig. 5*A*); (ii) they are sensitive to inhibition with the selective CRTH2 antagonist TRQ11238, which when given alone, does not induce any change in DMR (Fig. 5, *B* and *C*); and (iii) they are absent in cells transfected with empty pcDNA3.1 vector and challenged with PGD₂ or TRQ11238 (Fig. 5*C*). Real time DMR recordings show that Δ Ctail optical signatures were virtually superimposable to those of the WT receptor despite significantly lower cell surface expression (Fig. 5, *D–F*, and Fig. 2, *F* and *G*, for comparison). These results are in agreement with the GTP γ S binding data

but in apparent contrast to those obtained in second messenger IP and cAMP assays. Thus, monitoring receptor function in real time may imply that signaling superiority of Δ Ctail in IP and cAMP assays could be due to a lack of receptor desensitization, which would become apparent under those conditions that allow attenuation of a biological signal to occur in response to sustained agonist stimulation. In agreement with this notion, temporal resolution of IP production reveals that CRTH2 WT but not Δ Ctail is exposed to a molecular mechanism limiting further stimulation of downstream signaling and suggests that the C terminus plays a crucial role in determining the balance between ligand-stimulated activity and negative feedback inhibition (supplemental Fig. 2). Nevertheless, DMR data do confirm that the C terminus constrains maximum receptor activation since the magnitude of receptor signaling is (i) identical despite significantly lower expression of Δ Ctail (Fig. 5, *D–F*) and (ii) significantly increased for Δ Ctail when cells expressed approximately equal levels of cell surface CRTH2 WT and Δ Ctail, respectively (Fig. 6, *A* and *B*).

The CRTH2 C Terminus Is Required for PGD₂-mediated Recruitment of β -Arrestin2—It is well established that β -arrestin family members mediate desensitization of many GPCRs by uncoupling the stimulated receptors from their cognate G proteins (56, 57). To test whether CRTH2 WT and Δ Ctail differ in their ability to recruit arrestin proteins, both receptors were tested for physical association with β -arrestin2 using BRET assays. HEK293 cells transiently transfected with either CRTH2

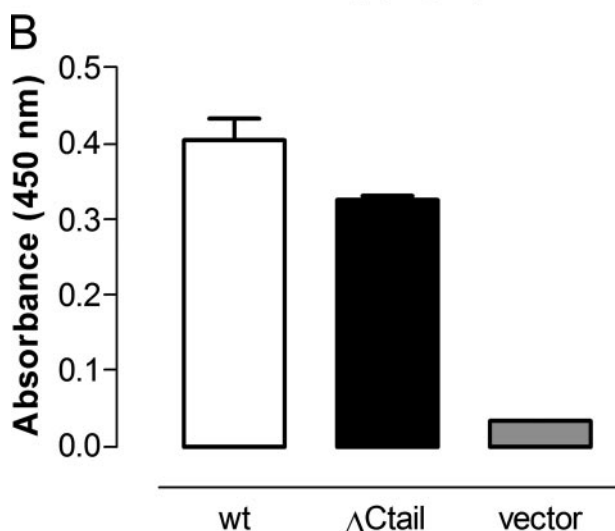
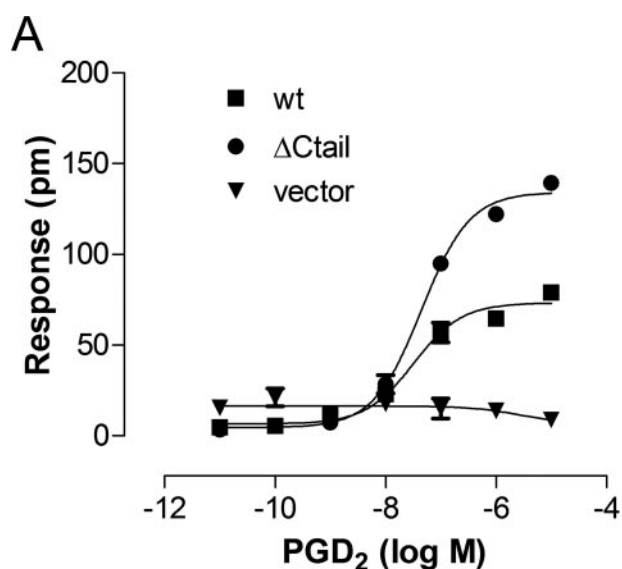


FIGURE 6. CRTH2 Δ Ctail is functionally superior in real time DMR assays. HEK293 cells were transiently transfected with 12 μ g of CRTH2 WT or 16 μ g of CRTH2 Δ Ctail plasmid DNA to express approximately equal amounts of both receptor constructs on the cell surface. Cells were analyzed in parallel for receptor functionality using DMR assays (A) and cell surface expression using ELISA assays (B). DMR assay details are identical to those in the legend of Fig. 5, D and E. Shown are mean values \pm S.E. of one experiment repeated on four different occasions.

WT or Δ Ctail fused in frame to *Renilla* luciferase (energy donor) and β -arrestin2-GFP2 (energy acceptor) were stimulated with increasing concentrations of PGD₂, and BRET was monitored. PGD₂ induced robust arrestin recruitment by CRTH2 WT, whereas the ability to recruit arrestin was lost by C-terminal truncation (Fig. 7). These data define the C terminus as the major site for physical association with arrestin and imply that lack of arrestin recruitment by the Δ Ctail receptor might account for its inability to limit G protein signaling upon sustained agonist exposure (compare Fig. 4, A and B, and supplemental Fig. 2).

CRTH2 Is Not Phosphorylated upon Agonist Exposure—We have previously reported that CRTH2 upon stimulation with PGD₂ recruits β -arrestin2 in a predominantly G protein-independent manner (7). Since CRTH2 recruits arrestin independently of G protein activation, we investigated whether phospho-

Silencing of CRTH2 Signaling by Its C-terminal Tail

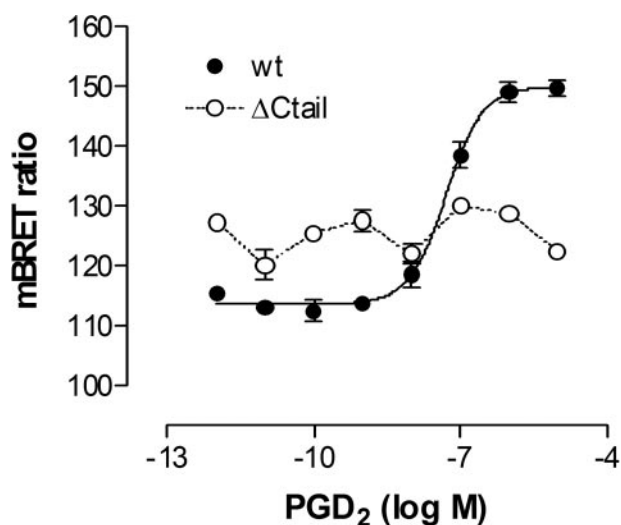


FIGURE 7. CRTH2 WT but not Δ Ctail recruits β -arrestin2 upon PGD₂ stimulation. HEK293 cells transiently transfected with β -arrestin-GFP2 and CRTH2-Rluc were exposed to increasing concentrations of PGD₂, and agonist-mediated increases in BRET were recorded. mBRET ratios were calculated as described under "Experimental Procedures." Shown are means \pm S.E. of triplicate determinations of one experiment repeated on four separate occasions.

rylation is a prerequisite for arrestin binding. HEK293 cells transiently expressing FLAG-tagged versions of the receptors were metabolically labeled with ³³P_i and stimulated with either PGD₂ or the synthetic agonist Indomethacin. Interestingly, neither basal nor agonist-mediated phosphorylation was detected with a highly sensitive phosphor imager, although both proteins could be visualized with the expected apparent molecular mass bands (~40 versus ~35 kDa) (Fig. 8). This finding was rather surprising, but the same technologies and similar experimental conditions have previously been applied successfully to detect phosphorylation of other proteins, including GPCRs (32, 34, 58–60). This suggests that CRTH2 phosphorylation should have been detected if it had occurred. In agreement with this notion, a positive control for phosphorylation, ASAP1 (32), was successfully phosphorylated in the same experiment. Thus, CRTH2 appears to represent a receptor that utilizes arrestin recruitment but not receptor phosphorylation as a negative feedback mechanism to limit downstream signaling.

Despite Its Inability to Recruit β -Arrestin2, CRTH2 Δ Ctail Remains Competent to Internalize upon Agonist Exposure—Since CRTH2 WT but not Δ Ctail is capable of recruiting β -arrestin2 to the plasma membrane and many receptors internalize in an arrestin-dependent manner, we sought to determine whether the tail-deleted receptor had lost the ability to internalize in response to agonist stimulation. Importantly, lack of internalization of Δ Ctail could also contribute to increased functional responsiveness upon agonist challenge and thus explain the divergent signaling properties of both receptors. HEK293 cells stably expressing CRTH2 WT or Δ Ctail were incubated with anti-FLAG M1 antibody to label surface receptors only. The cells were then stimulated with 1 μ M PGD₂ for 30 min, and cellular distribution of receptors was visualized by confocal imaging. Unexpectedly, upon stimulation with PGD₂, immunofluorescence was observed within the cells for both CRTH2 WT and the tail-truncated mutant (Fig. 9A). In fact,

Silencing of CRTH2 Signaling by Its C-terminal Tail

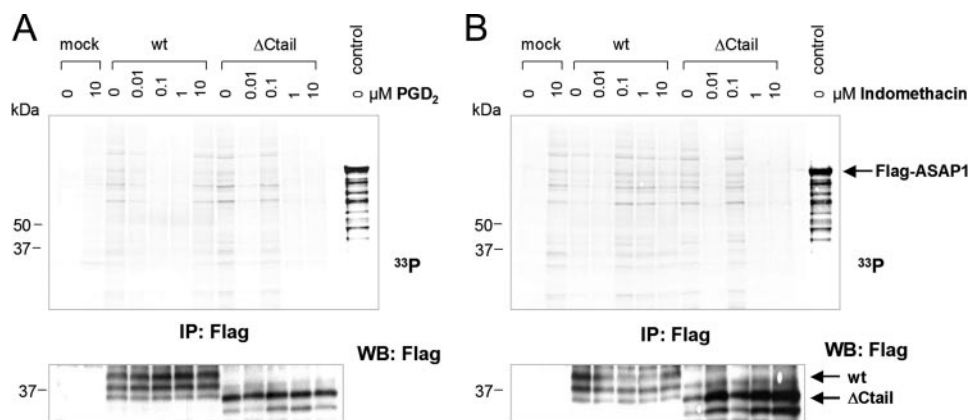


FIGURE 8. CRTH2 WT and CRTH2 Δ Ctail are not phosphorylated upon agonist stimulation. HEK293T cells grown on 6-well plates were transfected with 1.5 μ g/well of FLAG-tagged CRTH2 WT, Δ Ctail, or a FLAG-tagged control protein known to be phosphorylated (FLAG-ASAP1). After labeling with 0.625 mCi/ml 33 P-phosphate for 6 h, cells were stimulated with the indicated PGD₂ (A) and indomethacin (B) concentrations for 5 min and lysed, and FLAG-tagged proteins were isolated by immunoprecipitation using anti-FLAG-Sepharose beads. Following SDS-PAGE and transfer onto nitrocellulose membranes, radiolabeled proteins were analyzed using a phosphor imager (top). To control for proper immunoprecipitation, membranes were subsequently probed with an anti-FLAG antibody (bottom), and the expected molecular weight bands for WT and Δ Ctail were detected.

Δ Ctail even appeared to exhibit enhanced receptor internalization as compared with the wild type receptor. Similar results were obtained when internalization was quantified using Biotin protection assays (Fig. 9B). Thus, lack of arrestin recruitment, but not lack of agonist-mediated internalization, may explain the functional superiority of Δ Ctail.

PGD₂-mediated ERK1/2 Activation by CRTH2 Requires Coupling to G α_i Proteins and EGF Receptor Transactivation but Does Not Involve Arrestin Proteins or Protein Kinase C—It is well established that GPCRs are connected to MAPK signaling pathways through G α_i protein stimulation but in parallel also through a nonclassical, G protein-independent, arrestin-dependent way (61–64). Since CRTH2 is coupled to G α_i -type G proteins and capable of recruiting arrestin without prior G α_i activation (7), we tested both mechanisms of CRTH2-dependent MAPK activation and whether the C-terminal tail also constrains this downstream signaling event similar to its impact on G α_i activation. HEK293 cells stably expressing CRTH2 WT or Δ Ctail were treated with 10 μ M PGD₂ in the absence and presence of various pharmacological inhibitors, and ERK1/2 phosphorylation was measured using Western blot analysis of whole cell lysates with phospho-ERK-specific antibodies (Fig. 10). We found CRTH2-stimulated ERK1/2 activation to be (i) G α_i -dependent, since it is sensitive to PTX treatment; (ii) arrestin-independent, since Δ Ctail remains competent to induce ERK1/2 phosphorylation and since the CRTH2-specific arrestin translocation inhibitor 27868 (compound 1 in Ref. 7) does not impair ERK activation; and (iii) protein kinase C- and Src-independent, since the inhibitors GF109203X and PP2, respectively, are without effect on ERK phosphorylation but (iv) partly dependent on EGF receptor transactivation due to decreased ERK1/2 phosphorylation in the presence of the EGF receptor tyrosine kinase inhibitor Iressa. Despite lower surface expression of Δ Ctail (Fig. 2, F and G), similar intensity of ERK activation was observed for both receptors, suggesting that the C terminus also constrains engagement of

the ERK signaling cascade similar to constraining G α_i signaling.

The C Terminus of CRTH2 Does Not Determine G Protein Signaling Specificity—To investigate if the tail of CRTH2 also acts as a G protein signaling specificity filter and whether signaling to alternative G α proteins may be similarly enhanced as compared with G α_i signaling, HEK293 cells transiently transfected with CRTH2 WT or Δ Ctail, respectively, were tested for their ability to engage the three major G protein signaling pathways: G α_i , G α_s , and G α_q . To analyze and compare signaling capabilities of the wild type and mutant receptor, we took advantage of the novel DMR assays (Corning Epic[®] Biosensor), which allow monitoring of all three major G protein pathways in real

time within a single assay platform (54, 55). In addition, classical second messenger and biochemical GTP γ S assays were performed to support and validate the optical signatures obtained in the DMR assays (Fig. 4 and data not shown). It was apparent from DMR assays that deletion of the receptor C terminus yields optical signatures similar to those obtained for CRTH2 WT, suggesting that the engaged signaling pathways for WT and Δ Ctail are identical and reflect stimulation of G $\alpha_{i/o}$ proteins (Fig. 11A; compare also optical recordings in Fig. 5, D and E). In agreement with this notion, both signatures were abrogated in the presence of PTX, indicating that they result from G $\alpha_{i/o}$ activation (compare Figs. 5A and 11A). Furthermore, neither CRTH2 WT nor Δ Ctail were competent to engage with G α_s or G α_q signaling cascades, since no apparent activation of the latter pathways can be detected in the optical signatures. For means of comparison, optical signatures obtained upon stimulating the G α_s and G α_q signaling cascades are also depicted (Fig. 11, B and C). Our data clearly show that the receptor C terminus attenuates maximum receptor activation but does not carry any information to activate G proteins selectively.

DISCUSSION

G protein-coupled receptors are endowed with C termini that vary greatly in length and sequence. In many cases, C termini serve as docking sites for regulatory proteins, such as those of the arrestin family (65, 66). However, in many instances, tails appear to be dispensable, or of only modest relevance for G protein coupling (42, 67, 68). The most intriguing finding revealed by our study therefore is that the C terminus of CRTH2 is utilized as a molecular brake to limit the extent of CRTH2-triggered cellular responses. In fact, it is conceivable that the C-terminal tail prevents the heptahelical core of CRTH2 from engagement with G α_i and its downstream signaling cascade.

Recently, the second extracellular loop domain of the C5a receptor, the closest phylogenetic neighbor of CRTH2, was discovered as a negative regulator of receptor function, most likely

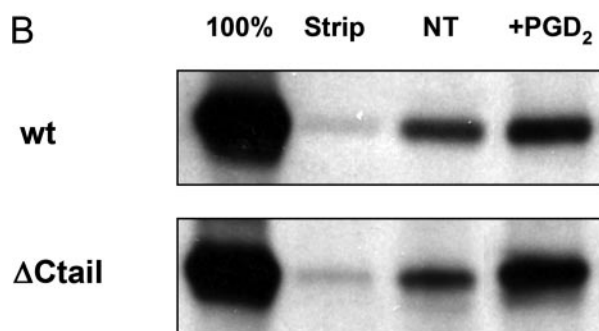
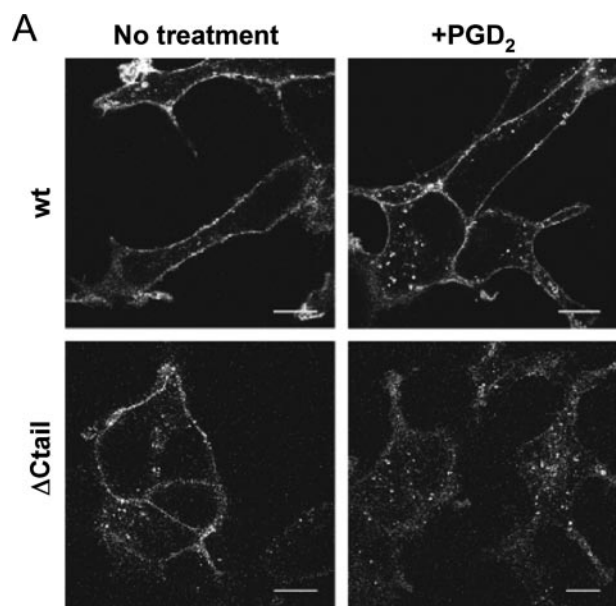


FIGURE 9. CRTH2 Δ Ctail is incompetent to recruit β -arrestin2 but remains competent to internalize. A, HEK293 cells stably expressing either CRTH2 WT (top) or CRTH2 Δ C-tail (bottom) fused to an N-terminal FLAG tag, were "antibody-fed" for 30 min, followed by 30 min of either no treatment (left) or incubation with $10 \mu\text{M}$ PDG₂ (right). All cells were then permeabilized, immunostained with a fluorescent secondary antibody, and imaged by confocal microscopy. Scale bar, $10 \mu\text{m}$. B, biotinylation protection assay performed on the same clones as used in A. Cells were treated with membrane-impermeable biotin for 30 min at 4°C labeling only cell surface receptors (100%). The cells were subsequently incubated for 20 min at 37°C before adding $10 \mu\text{M}$ PDG₂ or left untreated (NT) for another 30 min. Noninternalized, surface-bound biotin was stripped away (Strip), and receptors were immunoprecipitated, subjected to Western blot, and visualized using a streptavidin overlay. The blots are representative of two independent experiments.

by stabilizing the inactive receptor conformation (69). Our study identified the CRTH2 C terminus as a key determinant that constrains receptor activation. This notion is supported by the fact that the tail-deleted receptor shows higher affinity toward the agonist PDG₂ (Fig. 2, D and F) and that it paradoxically displays enhanced signaling in a variety of functional assays monitoring activation of G protein-dependent pathways (Figs. 4–6 and 10). As such, our results highlight the role of the C terminus in allosterically regulating CRTH2 and thus provide evidence that negative regulation of GPCR function is not only brought about by kinase-mediated phosphorylation and arrestin recruitment but also by the receptor itself. Hence, a receptor can take advantage of its C-terminal tail to sterically interdict coupling to G proteins.

C-terminal serines and threonines have been implicated in regulating GPCR desensitization and internalization. Princi-

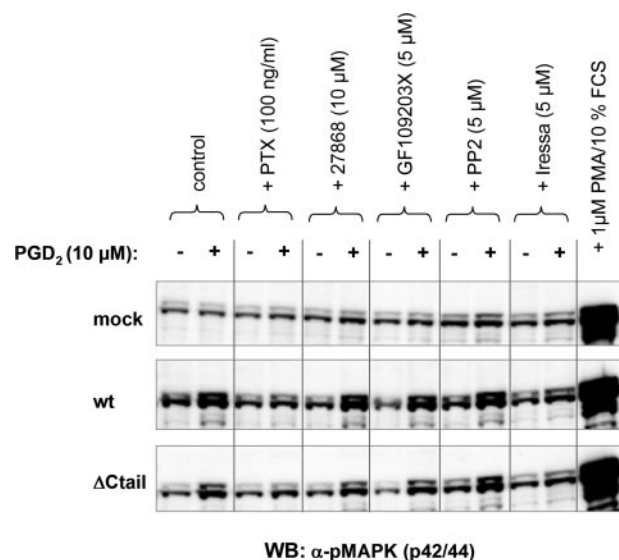


FIGURE 10. The CRTH2 C terminus also constrains receptor signaling to the ERK1/2 cascade. HEK293 cells expressing CRTH2 WT or Δ Ctail, were grown on 10-cm tissue culture dishes and incubated in the absence of serum for 16 h. Cells were then treated with the indicated inhibitors for 1 h (except for PTX that was present for 16 h) and then challenged with $10 \mu\text{M}$ PDG₂ for 10 min. Cells were lysed, and proteins were separated by SDS-PAGE and transferred onto nitrocellulose membranes. Subsequently, the activation of p42/44 MAPK (ERK1/2) was assessed using a phospho-specific antibody. Parental, nontransfected HEK293 cells served as control for endogenous PDG₂ receptors (mock) and stimulation with $1 \mu\text{M}$ phorbol 12-myristate 13-acetate and 10% fetal calf serum (FCS) was used to obtain maximal p42/44 MAPK activation. WB, Western blot.

pally, upon receptor activation, these residues are phosphorylated by G protein-coupled receptor kinases and/or second messenger-dependent kinases, which facilitate β -arrestin binding and can lead to both G protein uncoupling and internalization by targeting receptors to clathrin-coated pits (70–72). Although the C terminus of CRTH2 is spiked with potential phosphorylation sites, neither agonist-dependent nor constitutive phosphorylation could be detected (Fig. 8). Thus, CRTH2 lacks the classical mechanism for negative feedback regulation that is operative for the majority of GPCRs (66, 70–72). It is therefore tempting to propose that lack of negative regulation of CRTH2 signaling through phosphorylation may be compensated by the ability of the C terminus to constrain maximum receptor activation. As such, CRTH2 appears to use an up to now rather unappreciated strategy to limit its own signaling. At present, however, we cannot rule out the possibility that the C terminus is directly involved in interaction with an unknown regulatory protein and that this interaction could impose a similar limitation onto receptor signaling.

Another plausible explanation accounting for the enhanced G protein signaling capacity of the tail-deleted CRTH2 receptor could be its inability to undergo ligand-mediated receptor internalization. Unexpectedly, however, CRTH2 Δ Ctail remained competent to undergo both constitutive and agonist-mediated internalization (Fig. 9). In fact, lack of the C-terminal domain rather facilitated both internalization phenomena. Hence, this internalization phenotype would be counterproductive to efficient signal transduction as observed for Δ Ctail and cannot explain its functional superiority as compared with the WT receptor. Interestingly, CRTH2 Δ Ctail internalizes

Silencing of CRTH2 Signaling by Its C-terminal Tail

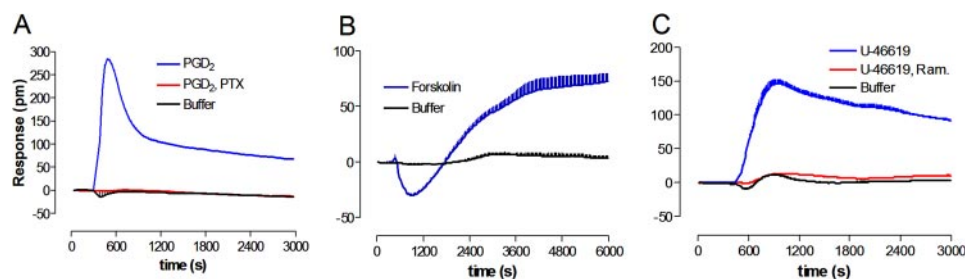


FIGURE 11. The CRTH2 C terminus does not control G protein coupling specificity of the receptor. A, HEK293 cells stably expressing CRTH2 Δ Ctail were challenged with 100 nM PGD₂, and receptor signaling was monitored in real time using DMR on the Corning Epic[®] biosensor. Overnight treatment (18 h) of cells with 100 ng/ml PTX abrogated the specific PGD₂ optical signature, indicating its G $\alpha_{i/o}$ nature. B, optical signature obtained upon stimulation of the G α_s cascade using 100 μ M forskolin in naive HEK293 cells. C, optical signature obtained upon stimulation of the G α_q cascade with a 1 μ M concentration of the thromboxane agonist U46619 in naive HEK293 cells. U46619 activation was completely abolished when cells were preincubated with a 10 μ M concentration of the thromboxane/CRTH2 receptor antagonist ramatroban (Ram.). U46619 activation was insensitive to PTX pretreatment (data not shown).

without being competent to physically associate with β -arrestin2 (Fig. 7). CRTH2 therefore represents a receptor, which is not only competent to internalize without prior phosphorylation but also without prior arrestin recruitment. A similar observation has also been made for the muscarinic M2 receptor (73, 74) and for selected phosphorylation-deficient mutants of the somatostatin sst2A receptor, which remain competent to internalize despite their inability to undergo ligand-mediated phosphorylation and arrestin recruitment, respectively (75).

Although β -arrestin2 recruitment is not necessary for CRTH2 internalization, PGD₂ stimulation induces arrestin translocation. However, this process does not require prior receptor phosphorylation. Phosphorylation-independent arrestin recruitment has recently also been observed for β_2 -adrenergic, angiotensin II AT1, and parathyroid hormone receptors (76). Our data therefore suggest that arrestin translocation and receptor phosphorylation may be completely separable molecular events and provide additional support for a model in which multiple receptor conformations possess distinct signaling properties that are differentially regulated.

Binding of arrestin proteins to phosphorylated receptors has long been considered as a means by which G protein activation is turned off. Recent evidence, however, indicates that arrestin binding may also serve as a parallel pathway for signal transduction, particularly for initiation of the MAPK signaling cascade (56). We have recently demonstrated that CRTH2 is also competent to recruit arrestin proteins but that this process does not require G protein activation (7). Herein, we demonstrate that CRTH2 is competent to engage with MAPK ERK1/2 signaling but that activation of this pathway is accomplished through G α_i , but not arrestin proteins. Hence, CRTH2 appears to recruit arrestin solely for desensitization purposes but not for propagating downstream signaling to the ERK1/2 cascade. We cannot rule out, however, the possibility that any yet unknown GPCR-mediated signaling events occur as a consequence of arrestin recruitment and that arrestin recruitment does not only serve the purpose of turning off receptor signaling. Nevertheless, the inability of the Δ Ctail to physically interact with β -arrestin2 may likely contribute to the enhanced signaling capacity of this receptor variant.

Recently, a new cardioprotective signaling pathway has been identified for the β_1 -adrenergic receptor utilizing arrestin proteins for transactivation of the EGF receptor that in turn induces MAPK activation (77). Our study revealed that CRTH2-mediated ERK1/2 stimulation resulted, at least in part, from EGF receptor transactivation, as evidenced by using the EGF receptor tyrosine kinase-specific inhibitor Iressa (Fig. 10). However, we can rule out involvement of arrestin proteins in EGF receptor transactivation, since both CRTH2 WT and Δ Ctail, the latter incompetent to

recruit arrestin, remain competent to engage the ERK1/2 pathway. Furthermore, the presence of PTX, an inhibitor of G $\alpha_{i/o}$ protein function, abrogated ERK phosphorylation, whereas Iressa only partly diminished it. Since EGF receptor transactivation is a downstream event of G α_i signaling, intrinsic inhibition of CRTH2 function is also operative for this branch of the kinase signaling network.

In summary, the experiments described herein provide the first detailed investigation of the role of the CRTH2 C terminus in receptor localization and signaling. Our data show that the C terminus is critically important for membrane localization and that it drives recruitment of β -arrestin2. Concurrently, the tail acts as an inhibitor of G α_i and its downstream signaling cascade. CRTH2 is not detectably phosphorylated; nor does it require phosphorylation for arrestin recruitment or arrestin recruitment for internalization. As such, our study reveals that the molecular mechanisms governing CRTH2 receptor signaling and function are distinct from those characteristic for many members of the rhodopsin family of GPCRs.

Acknowledgment—We are grateful to Corning for providing the Epic Biosensor.

REFERENCES

1. Hata, A. N., and Breyer, R. M. (2004) *Pharmacol. Ther.* **103**, 147–166
2. Kostenis, E., and Ulven, T. (2006) *Trends Mol. Med.* **12**, 148–158
3. Pettipher, R., Hansel, T. T., and Armer, R. (2007) *Nat. Rev.* **6**, 313–325
4. Lewis, R. A., Soter, N. A., Diamond, P. T., Austen, K. F., Oates, J. A., and Roberts, L. J., II (1982) *J. Immunol.* **129**, 1627–1631
5. Boie, Y., Sawyer, N., Slipetz, D. M., Metters, K. M., and Abramovitz, M. (1995) *J. Biol. Chem.* **270**, 18910–18916
6. Hirai, H., Tanaka, K., Yoshie, O., Ogawa, K., Kenmotsu, K., Takamori, Y., Ichimasa, M., Sugamura, K., Nakamura, M., Takano, S., and Nagata, K. (2001) *J. Exp. Med.* **193**, 255–261
7. Mathiesen, J. M., Ulven, T., Martini, L., Gerlach, L. O., Heinemann, A., and Kostenis, E. (2005) *Mol. Pharmacol.* **68**, 393–402
8. Bohm, E., Sturm, G. J., Weiglhofer, I., Sandig, H., Shichijo, M., McNamee, A., Pease, J. E., Kollroser, M., Peskar, B. A., and Heinemann, A. (2004) *J. Biol. Chem.* **279**, 7663–7670
9. Royer, J. F., Schratl, P., Lorenz, S., Kostenis, E., Ulven, T., Schuligoi, R., Peskar, B. A., and Heinemann, A. (2007) *Allergy* **62**, 1401–1409
10. Yoshimura-Uchiyama, C., Iikura, M., Yamaguchi, M., Nagase, H., Ishii, A., Matsushima, K., Yamamoto, K., Shichijo, M., Bacon, K. B., and Hirai, K.

- (2004) *Clin. Exp. Allergy* **34**, 1283–1290
11. Almishri, W., Cossette, C., Rokach, J., Martin, J. G., Hamid, Q., and Powell, W. S. (2005) *J. Pharmacol. Exp. Ther.* **313**, 64–69
 12. Monneret, G., Cossette, C., Gravel, S., Rokach, J., and Powell, W. S. (2003) *J. Pharmacol. Exp. Ther.* **304**, 349–355
 13. Shichijo, M., Sugimoto, H., Nagao, K., Inbe, H., Encinas, J. A., Takeshita, K., Bacon, K. B., and Gantner, F. (2003) *J. Pharmacol. Exp. Ther.* **307**, 518–525
 14. Satoh, T., Moroi, R., Aritake, K., Urade, Y., Kanai, Y., Sumi, K., Yokozeki, H., Hirai, H., Nagata, K., Hara, T., Utsuyama, M., Hirokawa, K., Sugamura, K., Nishioka, K., and Nakamura, M. (2006) *J. Immunol.* **177**, 2621–2629
 15. Spik, I., Brenuchon, C., Angeli, V., Staumont, D., Fleury, S., Capron, M., Trottein, F., and Dombrowicz, D. (2005) *J. Immunol.* **174**, 3703–3708
 16. Takeshita, K., Yamasaki, T., Nagao, K., Sugimoto, H., Shichijo, M., Gantner, F., and Bacon, K. B. (2004) *Int. Immunol.* **16**, 947–959
 17. Uller, L., Mathiesen, J. M., Alenmyr, L., Korsgren, M., Ulven, T., Hogberg, T., Andersson, G., Persson, C. G., and Kostenis, E. (2007) *Respir. Res.* **8**, 16–25
 18. Lukacs, N. W., Berlin, A. A., Franz-Bacon, K., Sasik, R., Sprague, L. J., Ly, T. W., Hardiman, G., Boehme, S. A., and Bacon, K. B. (2008) *Am. J. Physiol.* **295**, L767–L779
 19. Shiraishi, Y., Asano, K., Niimi, K., Fukunaga, K., Wakaki, M., Kagyo, J., Takihara, T., Ueda, S., Nakajima, T., Oguma, T., Suzuki, Y., Shiomi, T., Sayama, K., Kagawa, S., Ikeda, E., Hirai, H., Nagata, K., Nakamura, M., Miyasho, T., and Ishizaka, A. (2008) *J. Immunol.* **180**, 541–549
 20. Tajima, T., Murata, T., Aritake, K., Urade, Y., Hirai, H., Nakamura, M., Ozaki, H., and Hori, M. (2008) *J. Pharmacol. Exp. Ther.* **326**, 493–501
 21. Wang, J., Xu, Y., Zhao, H., Sui, H., Liang, H., and Jiang, X. (2008) *Mol. Biol. Rep.*, in press
 22. Yamamoto, M., Okano, M., Fujiwara, T., Kariya, S., Higaki, T., Nagatsuka, H., Tsujigami, H., Yamada, M., Yoshino, T., Urade, Y., and Nishizaki, K. (2008) *Int. Arch. Allergy Immunol.* **148**, 127–136
 23. Hata, A. N., Lybrand, T. P., and Breyer, R. M. (2005) *J. Biol. Chem.* **280**, 32442–32451
 24. Ulven, T., Gallen, M. J., Nielsen, M. C., Merten, N., Schmidt, C., Mohr, K., Trankle, C., and Kostenis, E. (2007) *Bioorg. Med. Chem. Lett.* **17**, 5924–5927
 25. Kostenis, E., Martini, L., Ellis, J., Waldhoer, M., Heydorn, A., Rosenkilde, M. M., Norregaard, P. K., Jorgensen, R., Whistler, J. L., and Milligan, G. (2005) *J. Pharmacol. Exp. Ther.* **313**, 78–87
 26. Wise, A., Foord, S. M., Fraser, N. J., Barnes, A. A., Elshourbagy, N., Eilert, M., Ignar, D. M., Murdock, P. R., Steplewski, K., Green, A., Brown, A. J., Dowell, S. J., Szekeres, P. G., Hassall, D. G., Marshall, F. H., Wilson, S., and Pike, N. B. (2003) *J. Biol. Chem.* **278**, 9869–9874
 27. Hosoi, T., Koguchi, Y., Sugikawa, E., Chikada, A., Ogawa, K., Tsuda, N., Suto, N., Tsunoda, S., Taniguchi, T., and Ohnuki, T. (2002) *J. Biol. Chem.* **277**, 31459–31465
 28. Wittamer, V., Franssen, J. D., Vulcano, M., Mirjolet, J. F., Le Poul, E., Migeotte, I., Brezillon, S., Tyldesley, R., Blanpain, C., Detheux, M., Mantovani, A., Sozzani, S., Vassart, G., Parmentier, M., and Communi, D. (2003) *J. Exp. Med.* **198**, 977–985
 29. Mathiesen, J. M., Christopoulos, A., Ulven, T., Royer, J. F., Campillo, M., Heinemann, A., Pardo, L., and Kostenis, E. (2006) *Mol. Pharmacol.* **69**, 1441–1453
 30. Fang, Y., Ferrie, A. M., Fontaine, N. H., and Yuen, P. K. (2005) *Anal. Chem.* **77**, 5720–5725
 31. Fang, Y., Ferrie, A. M., Fontaine, N. H., Mauro, J., and Balakrishnan, J. (2006) *Biophys. J.* **91**, 1925–1940
 32. Kruljac-Letic, A., Moelleken, J., Kallin, A., Wieland, F., and Blaukat, A. (2003) *J. Biol. Chem.* **278**, 29560–29570
 33. Blaukat, A., Alla, S. A., Lohse, M. J., and Muller-Esterl, W. (1996) *J. Biol. Chem.* **271**, 32366–32374
 34. Blaukat, A., Pizard, A., Breit, A., Wernstedt, C., Alhenc-Gelas, F., Muller-Esterl, W., and Dikic, I. (2001) *J. Biol. Chem.* **276**, 40431–40440
 35. Delhay, M., Gravot, A., Ayinde, D., Niedergang, F., Alizon, M., and Brelot, A. (2007) *Mol. Pharmacol.* **72**, 1497–1507
 36. Pankevych, H., Korkhov, V., Freissmuth, M., and Nanoff, C. (2003) *J. Biol. Chem.* **278**, 30283–30293
 37. Levoe, A., Dam, J., Ayoub, M. A., Guillaume, J. L., Couturier, C., Delagrè, P., and Jockers, R. (2006) *EMBO J.* **25**, 3012–3023
 38. Hoare, S., Copland, J. A., Strakova, Z., Ives, K., Jeng, Y. J., Hellmich, M. R., and Soloff, M. S. (1999) *J. Biol. Chem.* **274**, 28682–28689
 39. Kang, D. S., and Leeb-Lundberg, L. M. (2002) *Mol. Pharmacol.* **62**, 281–288
 40. Labasque, M., Reiter, E., Becamel, C., Bockaert, J., and Marin, P. (2008) *Mol. Biol. Cell* **19**, 4640–4650
 41. McCulloch, C. V., Morrow, V., Milasta, S., Comerford, I., Milligan, G., Graham, G. J., Isaacs, N. W., and Nibbs, R. J. (2008) *J. Biol. Chem.* **283**, 7972–7982
 42. Estall, J. L., Koehler, J. A., Yusta, B., and Drucker, D. J. (2005) *J. Biol. Chem.* **280**, 22124–22134
 43. Tohgo, A., Choy, E. W., Gesty-Palmer, D., Pierce, K. L., Laporte, S., Oakley, R. H., Caron, M. G., Lefkowitz, R. J., and Luttrell, L. M. (2003) *J. Biol. Chem.* **278**, 6258–6267
 44. Cherezov, V., Rosenbaum, D. M., Hanson, M. A., Rasmussen, S. G., Thian, F. S., Kobilka, T. S., Choi, H. J., Kuhn, P., Weis, W. I., Kobilka, B. K., and Stevens, R. C. (2007) *Science* **318**, 1258–1265
 45. Delos Santos, N. M., Gardner, L. A., White, S. W., and Bahouth, S. W. (2006) *J. Biol. Chem.* **281**, 12896–12907
 46. Jaakola, V. P., Griffith, M. T., Hanson, M. A., Cherezov, V., Chien, E. Y., Lane, J. R., Ijzerman, A. P., and Stevens, R. C. (2008) *Science* **322**, 1211–1217
 47. Palczewski, K., Kumasaka, T., Hori, T., Behnke, C. A., Motoshima, H., Fox, B. A., Le Trong, I., Teller, D. C., Okada, T., Stenkamp, R. E., Yamamoto, M., and Miyano, M. (2000) *Science* **289**, 739–745
 48. Sano, T., Ohyama, K., Yamano, Y., Nakagomi, Y., Nakazawa, S., Kikyo, M., Shirai, H., Blank, J. S., Exton, J. H., and Inagami, T. (1997) *J. Biol. Chem.* **272**, 23631–23636
 49. Katragadda, M., Maciejewski, M. W., and Yeagle, P. L. (2004) *Biochim. Biophys. Acta* **1663**, 74–81
 50. Okuno, T., Ago, H., Terawaki, K., Miyano, M., Shimizu, T., and Yokomizo, T. (2003) *J. Biol. Chem.* **278**, 41500–41509
 51. Okuno, T., Yokomizo, T., Hori, T., Miyano, M., and Shimizu, T. (2005) *J. Biol. Chem.* **280**, 32049–32052
 52. Swift, S., Legger, A. J., Talavera, J., Zhang, L., Bohm, A., and Kuliopulos, A. (2006) *J. Biol. Chem.* **281**, 4109–4116
 53. Verzijl, D., Pardo, L., van Dijk, M., Grujthuijsen, Y. K., Jongejan, A., Timmerman, H., Nicholas, J., Schwarz, M., Murphy, P. M., Leurs, R., and Smit, M. J. (2006) *J. Biol. Chem.* **281**, 35327–35335
 54. Fang, Y., Frutos, A. G., and Verkleeren, R. (2008) *Combin. chem. High Throughput Screen.* **11**, 357–369
 55. Lee, P. H., Gao, A., van Staden, C., Ly, J., Salon, J., Xu, A., Fang, Y., and Verkleeren, R. (2008) *Assay Drug Dev. Technol.* **6**, 83–94
 56. Lefkowitz, R. J., and Shenoy, S. K. (2005) *Science* **308**, 512–517
 57. Reiter, E., and Lefkowitz, R. J. (2006) *Trends Endocrinol. Metab.* **17**, 159–165
 58. Kalatskaya, I., Schussler, S., Blaukat, A., Muller-Esterl, W., Jochum, M., Proud, D., and Faussner, A. (2004) *J. Biol. Chem.* **279**, 31268–31276
 59. Schermer, B., Hopker, K., Omran, H., Ghenoio, C., Fliegau, M., Fekete, A., Horvath, J., Kottgen, M., Hackl, M., Zschiedrich, S., Huber, T. B., Kramer-Zucker, A., Zentgraf, H., Blaukat, A., Walz, G., and Benzing, T. (2005) *EMBO J.* **24**, 4415–4424
 60. Torrecilla, I., Spragg, E. J., Poulin, B., McWilliams, P. J., Mistry, S. C., Blaukat, A., and Tobin, A. B. (2007) *J. Cell Biol.* **177**, 127–137
 61. Azzi, M., Charest, P. G., Angers, S., Rousseau, G., Kohout, T., Bouvier, M., and Pineyro, G. (2003) *Proc. Natl. Acad. Sci. U. S. A.* **100**, 11406–11411
 62. Baker, J. G., Hall, I. P., and Hill, S. J. (2003) *Mol. Pharmacol.* **64**, 1357–1369
 63. Hall, R. A., and Lefkowitz, R. J. (2002) *Circ. Res.* **91**, 672–680
 64. Wei, H., Ahn, S., Shenoy, S. K., Karnik, S. S., Hunyady, L., Luttrell, L. M., and Lefkowitz, R. J. (2003) *Proc. Natl. Acad. Sci. U. S. A.* **100**, 10782–10787
 65. Bockaert, J., Marin, P., Dumuis, A., and Fagni, L. (2003) *FEBS Lett.* **546**, 65–72
 66. Lefkowitz, R. J., Rajagopal, K., and Whalen, E. J. (2006) *Mol. Cell* **24**, 643–652
 67. Budd, D. C., McDonald, J., Emsley, N., Cain, K., and Tobin, A. B. (2003) *The J. Biol. Chem.* **278**, 19565–19573

Silencing of CRTH2 Signaling by Its C-terminal Tail

68. Wess, J., Bonner, T. I., and Brann, M. R. (1990) *Mol. Pharmacol.* **38**, 872–877
69. Klco, J. M., Wiegand, C. B., Narzinski, K., and Baranski, T. J. (2005) *Nat. Struct. Mol. Biol.* **12**, 320–326
70. DeWire, S. M., Ahn, S., Lefkowitz, R. J., and Shenoy, S. K. (2007) *Annu. Rev. Physiol.* **69**, 483–510
71. Ferguson, S. S. (2007) *Trends Pharmacol. Sci.* **28**, 173–179
72. Gurevich, E. V., and Gurevich, V. V. (2006) *Genome Biol.* **7**, 236
73. Lee, K. B., Ptasiński, J. A., Pals-Rylaarsdam, R., Gurevich, V. V., and Hosey, M. M. (2000) *J. Biol. Chem.* **275**, 9284–9289
74. Pals-Rylaarsdam, R., Gurevich, V. V., Lee, K. B., Ptasiński, J. A., Benovic, J. L., and Hosey, M. M. (1997) *J. Biol. Chem.* **272**, 23682–23689
75. Liu, Y., Steiniger, S. C., Kim, Y., Kaufmann, G. F., Felding-Habermann, B., and Janda, K. D. (2007) *Mol. Pharmaceutics* **4**, 435–447
76. Shukla, A. K., Violin, J. D., Whalen, E. J., Gesty-Palmer, D., Shenoy, S. K., and Lefkowitz, R. J. (2008) *Proc. Natl. Acad. Sci. U. S. A.* **105**, 9988–9993
77. Noma, T., Lemaire, A., Naga Prasad, S. V., Barki-Harrington, L., Tilley, D. G., Chen, J., Le Corvoisier, P., Violin, J. D., Wei, H., Lefkowitz, R. J., and Rockman, H. A. (2007) *J. Clin. Investig.* **117**, 2445–2458
78. Ballesteros, J. A., and Weinstein, H. (1995) *Methods Neurosci.* **25**, 366–428